Alteration of Organic Acid Metabolism in Arabidopsis Overexpressing the Maize C_4 NADP-Malic Enzyme Causes Accelerated Senescence during Extended Darkness[1][W]

Holger Fahnenstich[2], Mariana Saigo[2], Michaela Niessen, María I. Zanor, Carlos S. Andreo, Alisdair R. Fernie, María F. Drincovich, Ulf-Ingo Flügge, and Verónica G. Maurino*

Botanisches Institut, Universität zu Köln, 50931 Cologne, Germany (H.F., M.N., U.-I.F., V.G.M.); Centro de Estudios Fotosintéticos y Bioquímicos, Universidad Nacional de Rosario, 2000 Rosario, Argentina (M.S., C.S.A., M.F.D.); and Max-Planck-Institut für Molekulare Pflanzenphysiologie, 14474 Potsdam-Golm, Germany (M.I.Z., A.R.F.)

The full-length cDNA encoding the maize (*Zea mays*) C_4 NADP-malic enzyme was expressed in Arabidopsis (*Arabidopsis thaliana*) under the control of the cauliflower mosaic virus 35S promoter. Homozygous transgenic plants (MEm) were isolated with activities ranging from 6- to 33-fold of those found in the wild type. The transformants did not show any differences in morphology and development when grown in long days; however, dark-induced senescence progressed more rapidly in MEm plants compared to the wild type. Interestingly, senescence could be retarded in the transgenic lines by exogenously supplying glucose, sucrose, or malate, suggesting that the lack of a readily mobilized carbon source is likely to be the initial factor leading to the premature induction of senescence in MEm plants. A comprehensive metabolic profiling on whole rosettes allowed determination of approximately 80 metabolites during a diurnal cycle as well as following dark-induced senescence and during metabolic complementation assays. MEm plants showed no differences in the accumulation and degradation of carbohydrates with respect to the wild type in all conditions tested, but accumulated lower levels of intermediates used as respiratory substrates, prominently malate and fumarate. The data indicated that extremely low levels of malate and fumarate are responsible for the accelerated dark-induced senescence encountered in MEm plants. Thus, in prolonged darkness these metabolites are consumed faster than in the wild type and, as a consequence, MEm plants enter irreversible senescence more rapidly. In addition, the data revealed that both malate and fumarate are important forms of fixed carbon that can be rapidly metabolized under stress conditions in Arabidopsis.

Malate has a pivotal role in most plant organelles. Fluxes of malate between the different subcellular compartments are fast (Kalt et al., 1990), and many transport systems involved in interorganellar malate translocation have been described (Taniguchi et al., 2002; Emmerlich et al., 2003; Renné et al., 2003; Scheibe, 2004). Malate is furthermore involved in many physiological functions, such as (1) provision of NADH for nitrate reduction, (2) provision of carbon skeletons and NADPH for fatty acid biosynthesis, (3) support of photorespiration, (4) stomatal movement by regulation of osmotic pressure, (5) control of cellular pH, (6) redox homeostasis, and (7) transport and exchange of reduced equivalents between cellular compartments (Lance and Rustin, 1984). In leaves of C_3 plants, malate shows a diurnal rhythm, in which the level increases during the light period with a maximum at the end of the day and decreases during the night. Malate synthesis during the light period involves the sequential action of phospho*enol*pyruvate carboxylase (PEPC) and malate dehydrogenase (MDH). PEPC is an allosteric enzyme inhibited by malate, activated by Glc-6-P, and regulated by reversible phosphorylation of a conserved Ser residue near the N terminus of the protein (Nimmo, 2003). Phosphorylation reduces the sensitivity to malate and increases the sensitivity toward Glc-6-P. The phosphorylation state is regulated by PEPC kinase, which has been shown to be under circadian control in leaves of soybean (*Glycine max*), with maximal activity during the light period (Fontaine et al., 2002; Sullivan et al., 2005). These data suggest that phosphorylation of PEPC plays a role in the coordination of CO_2 fixation and carbon partitioning in photosynthetic organs. During the light period, when a certain threshold of cytosolic malate concentration is reached, malate is transported into the vacuole, where it accumulates (Gout et al., 1993). Recently, a vacuolar malate transporter (AttDT) was characterized and has

[1] This work was supported by the Deutsche Forschungsgemeinschaft (V.G.M.) and by Agencia Nacional de Promocion de Actividades Cientificas y Tecnologicas and CONICET.

[2] These authors contributed equally to the article.

* Corresponding author; e-mail v.maurino@uni-koeln.de.

The author responsible for distribution of materials integral to the findings presented in this article in accordance with the policy described in the Instructions for Authors (www.plantphysiol.org) is: Verónica G. Maurino (v.maurino@uni-koeln.de).

[W] The online version of this article contains Web-only data.

www.plantphysiol.org/cgi/doi/10.1104/pp.107.104455

been shown to have a major function in photosynthetically active tissues (Emmerlich et al., 2003; Hurth et al., 2005). In the dark, the activation state of PEPC declines, the flux of malate toward the vacuole is stopped, and the stored malic acid is released to be further metabolized by decarboxylation to pyruvate, which can be used as an energy source in the TCA cycle (Martinoia and Rentsch, 1994). On the other hand, excess malate can be converted to fumarate by fumarase. Since the cytoplasmic compartment is devoid of fumarase activity, a permanent movement of malate and fumarate molecules between the different cell compartments is required. Using ^{13}C NMR, it was shown that labeled malate synthesized by the sequence involving PEPC and MDH is further converted to fumarate by the mitochondrial fumarase in vivo (Gout et al., 1993). Moreover and consistent with this observation, transgenic tomato (*Solanum lycopersicum*) plants with a reduced expression of fumarase were characterized to have marginally elevated malate contents (Nunes-Nesi et al., 2007).

In plants, NADP-dependent malic enzyme (NADP-ME; EC 1.1.1.40) is found in both the cytosol and in plastids, where it catalyses the oxidative decarboxylation of malate yielding pyruvate and NADPH. The Arabidopsis (*Arabidopsis thaliana*) genome contains four genes encoding NADP-ME isoforms. AtNADP-ME1 to AtNADP-ME3 are cytosolic (V.G. Maurino, unpublished data), whereas AtNADP-ME4 is localized to plastids (Gerrard Wheeler et al., 2005). In maize (*Zea mays*), to date, cDNAs for two plastidic isoforms have been cloned and the corresponding proteins have been characterized (Rothermel and Nelson, 1989; Maurino et al., 2001; Detarsio et al., 2003; Saigo et al., 2004). Different biological roles for the C_3 isoforms were suggested, but only the isoforms with a characterized physiological function are the ones that take part in the C_4 and CAM photosynthetic metabolisms (Drincovich et al., 2001).

In this work, we present the generation and characterization of transgenic Arabidopsis plants overexpressing the maize C_4 NADP-ME (MEm lines), which offered a way to alter malate levels and to analyze the physiological consequences of the observed metabolic disturbance. The phenotype of these lines following extended darkness suggests a highly important role for both malate and fumarate in the primary metabolism of Arabidopsis. The combination of metabolite profiling and metabolic complementation assays allowed us to conclude that MEm transgenic plants entered dark-induced senescence more rapidly due to an accelerated depletion of carbon and energy sources.

RESULTS

Isolation and Genetic and Biochemical Characterization of Transgenic Arabidopsis Plants Expressing the Maize C_4 NADP-ME

The plasmid *35S:MEmC_4* was introduced into the Arabidopsis 'Columbia-0' genome, and primary (T1) transformants were selected for BASTA resistance and screened for the presence of the transgene by PCR analysis. Total leaf extracts of the selected plants were tested for NADP-ME activity at pH 8.0, the optimum pH of the C_4 maize isozyme (Maurino et al., 1996). Lines with NADP-ME activity higher than the wild type were subjected to a second round of selection. Ten individual T2 plants of each line were analyzed by PCR and NADP-ME activity was determined. Three lines (MEm2, MEm4, and MEm5) were selected and subjected to another BASTA selection to obtain non-segregating T3 transgenic lines. Leaf tissue from the homozygous T3 plants was extracted and analyzed for NADP-ME activity, SDS-PAGE, and immunoblotting. Line MEm5 showed the highest NADP-ME activity, with 33-fold more activity than the wild type, while lines MEm2 and MEm4 displayed 6- and 24-fold increases, respectively (Fig. 1A). An immunoreactive 62-kD band, which corresponds to the molecular mass of the mature maize C_4 NADP-ME, was detected in all transgenic lines by immunoblotting using specific antibodies (Fig. 1A, inset). Moreover, leaf extracts subjected to native gel electrophoreses and stained for NADP-ME activity showed a band of approximately 240 kD in all MEm lines (data not shown). The molecular mass of the active band corresponded to the tetrameric state of maize C_4 NADP-ME, indicating a correct assembly of the overexpressed enzyme.

To test if the 66-kD precursor protein of the maize C_4 NADP-ME encoded by the full-length cDNA is directed to plastids of C_3 plants, a chloroplast import assay was performed. The in vitro synthesized precursor was imported into spinach (*Spinacia oleracea*) chloroplasts and processed to a protein of approximately 62 kD (Fig. 1B). Thermolysin treatment of the chloroplasts after import resulted in the disappearance of the precursor protein, while a smaller protein, corresponding in size to the mature C_4 NADP-ME, remained intact (Fig. 1B). To confirm the proper intracellular localization of the overexpressed enzyme in vivo, leaf sections from all MEm transgenic lines were subjected to immunoassays using antibodies against the maize C_4 NADP-ME. The results showed that the mature NADP-ME is efficiently targeted to chloroplasts of the transgenic plants (Fig. 1C). Southern-blot analyses indicated that lines MEm2, MEm4, and MEm5 possessed only a single transgene copy (not shown).

Diurnal Effects of an Enhanced Chloroplastic NADP-ME Activity on Metabolite Levels

MEm lines grown in long days do not show any morphological or developmental alteration in comparison to the wild type (Fig. 2A). No differences in seed morphology, yield, and germination were observed between the transgenic lines and the wild type (not shown). Chlorophyll content (Fig. 2B), photosynthetic electron transport rates (not shown), and the F_V/F_M ratio (Fig. 2C) of the transformants were similar to those of the wild type, indicating that the photosynthetic performance

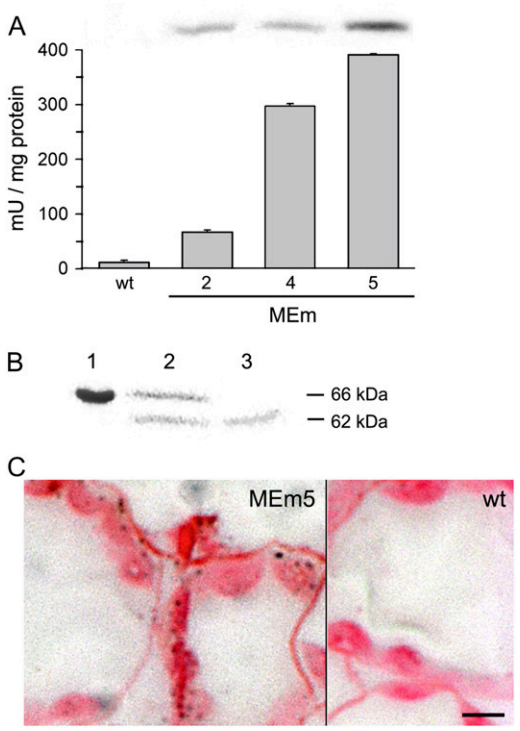

Figure 1. Analysis of maize C_4 NADP-ME expression in Arabidopsis. A, NADP-ME activity from leaf crude extracts of wild type (wt; 12 ± 3.4 mU/mg protein) and the transgenic lines MEm2, MEm4, and MEm5 (67 ± 3.4, 297 ± 4.5, and 391 ± 1.6 mU/mg protein, respectively) measured at pH 8.0. Inset, Immunoblot analysis of C_4 NADP-ME showing a reactive band in the transgenic lines. Errors bars indicate SD (n = 6). B, Chloroplast import assay of C_4 NADP-ME encoded by the full-length cDNA. Lane 1, 66-kD translational product synthesized in vitro. Lane 2, Intact washed chloroplast after import. Lane 3, Intact washed chloroplasts treated with thermolysin after import showing the 62-kD protected mature protein. C, Immunodetection of maize C_4 NADP-ME in a leaf section of the transgenic line MEm5 using specific antibodies. A section of the wild type incubated with the same antibodies showed no reaction. The bar represents 5 μm.

of the MEm lines was not affected under the given growth conditions. To investigate the influence of enhanced chloroplastic NADP-ME activity on leaf metabolism, a comprehensive metabolic analysis of extracts from rosettes harvested from 4-week-old plants grown in long days at different time points during a diurnal cycle was conducted. The levels of more than 80 metabolites were determined by gas chromatography (GC)-mass spectrometry (MS), and, additionally, the contents of sugars were measured photometrically.

With regard to carbohydrates, no differences in the levels or the pattern of accumulation of starch, Suc, Glc, and Fru were detected between the transgenic lines and the wild type during a long-day photoperiod (Supplemental Table S1).

All three MEm transformants analyzed displayed the same variations in the metabolic profiles when compared to the wild type. For ease of comparison, the data obtained for MEm4 are shown as representative for the MEm lines (Figs. 3 and 4; the whole data set is, however, available as supplemental material). As expected, the levels of malate, the substrate of the NADP-ME reaction, were dramatically reduced in the MEm transformants (Fig. 3). At the end of the dark and light periods, MEm leaves accumulated to 26% and 28% of the malate levels of the wild type, respectively. Fumarate levels mirrored those of malate. At the end of the night and light periods, MEm leaves accumulated 39% and 44% of the fumarate levels of the wild type, respectively (Fig. 3; Supplemental Table S2). Similar accumulation profiles were obtained for malate and fumarate during the light period. During the first part of the light period, a lag phase in the accumulation of both metabolites was observed, followed by an increased rate of accumulation that reached maximum levels at the end of the day. During the night, malate and fumarate were consumed in all lines, with malate contents decreasing continuously and reaching minimum levels at the end of the night period. Fumarate showed a different pattern of degradation. In all lines, a pronounced decrease of the fumarate level was observed after 1 h in darkness (Fig. 3). In the wild type, a subsequent accumulation up to levels similar to those found at the end of the day was observed, followed by a continuous decrease until the end of the night period. In contrast, in the MEm lines, the level was maintained during the next hours and then decreased to a low level until the end of the night period. Interestingly, the area of the fumarate peak detected in the gas chromatograms of the wild type indicated that, besides Suc, fumarate is the highest abundant metabolite in leaves of Arabidopsis during the light period. Contents of fumarate of 17.03 ± 1.26 μmol/mg fresh weight were determined in 4-week-old wild-type rosettes at the end of light period.

The levels of pyruvate, the direct product of the reaction catalyzed by NADP-ME, were increased in all transgenic lines; however, the pattern of the diurnal change was similar to that of the wild type (Fig. 3). At the end of the night period, the level of pyruvate in the MEm plants was 70% higher than that observed in the wild type, in which the pyruvate level peaked immediately after the light was switched on and decreased afterward (Fig. 3). MEm transformants showed a similar profile, while the highest level was about 2-fold higher than in the wild type. The pyruvate-derived amino acids Leu, Val, and, especially, Ala were also more abundant in the MEm plants and showed a similar pattern of accumulation as the wild type (Fig. 3).

The levels of the organic acids citrate, 2-oxoglutarate, and oxaloacetate were comparable in all lines (Fig. 3). Interestingly, succinate levels in the transgenic lines were significantly increased during the whole light period with respect to wild-type values, while in the second half of the night phase they were similar to those observed in the wild type (Fig. 3).

In the MEm transformants, the levels of Asp, Thr, Ile, and Met were decreased with respect to the wild type during the whole diurnal phase, except for Asp and Ile at the end of the night period, in which the

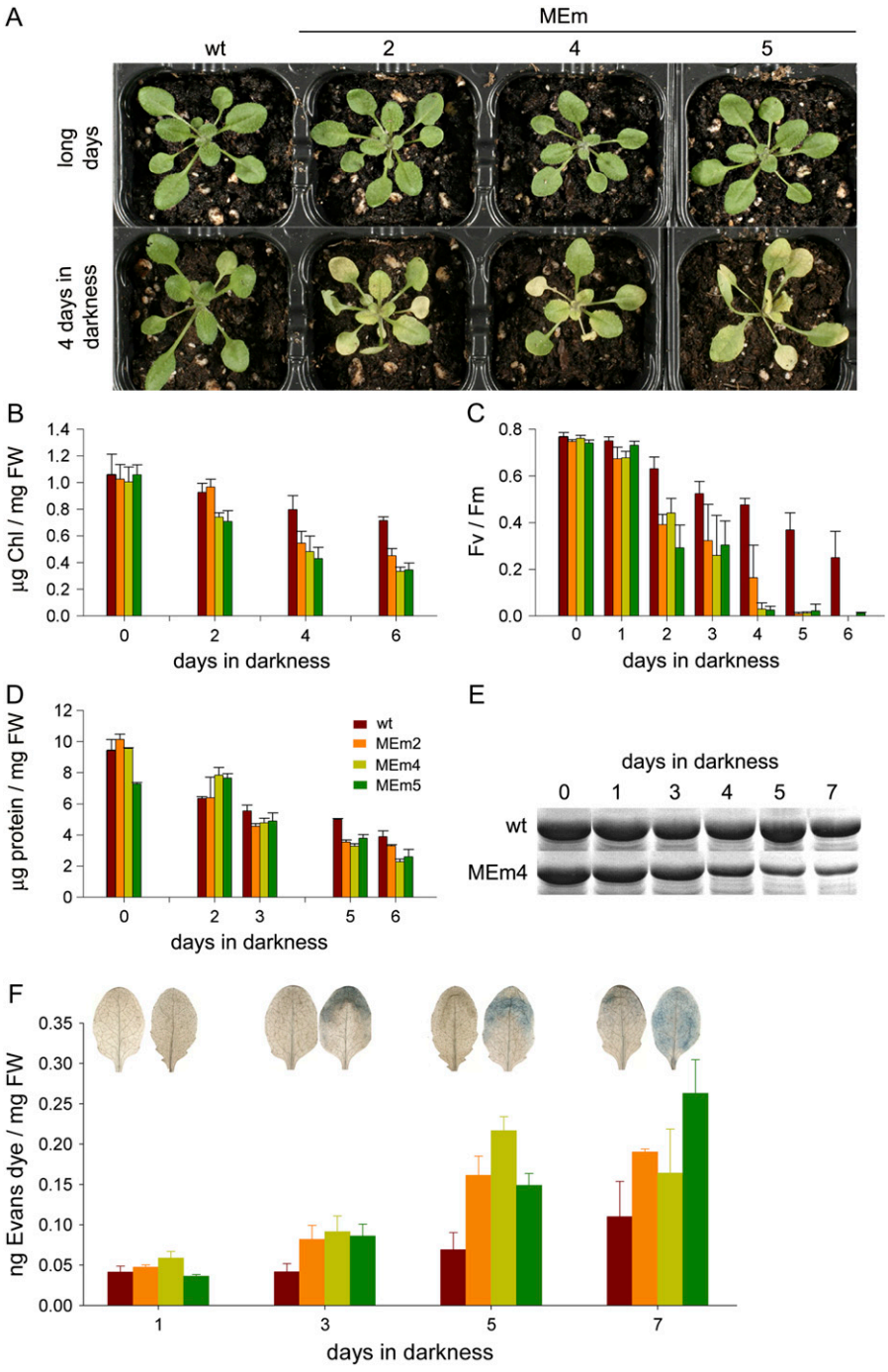

Figure 2. Phenotype of MEm transgenic lines and comparison of senescence parameters with the wild type. A, Images of 4-week-old wild type and transgenic lines grown in long days. The same plants were transferred to prolonged darkness and photographed after 4 d of treatment. B, Chlorophyll content. C, Maximum quantum yield of PSII (F_V/F_M). D, Total protein content. E, Accumulation of the 54-kD band of the Rubisco large subunit resolved by SDS-PAGE and stained with Coomassie Blue. F, Evans blue accumulation as indicator of cell death was measured spectrophotometrically in the wild type and MEm transformants at different times during extended darkness. Images of Evans blue-stained leaves from the wild type (on the left) and MEm line 4 (on the right) are shown. FW, Fresh weight. Error bars indicate SD ($n = 6$).

levels were similar to the wild type (Fig. 3; Supplemental Table S2). Asn and Lys, however, could be detected only in very low amounts, and no differences in their levels were observable between the MEm plants and the wild type (Supplemental Table S2).

Glu and GABA levels in the transgenics showed patterns similar to those in the wild type (Fig. 3). While the Glu levels remained lower than in the wild type throughout the diurnal period except for the end of the night, the content of GABA was enhanced at the end of the light period and decreased below wild-type values by the end of the dark phase. This elevated GABA content could be a result of enhanced synthesis from Glu, given that the oxaloacetate levels were also higher in the MEm plants at the same time points (Fig. 3). A similar pattern was observed for the levels of His, which is synthesized from Gln (Fig. 3).

Glc-6-P and Fru-6-P levels were closely related to each other during the diurnal cycle and similar patterns were found in the transgenic lines and the wild

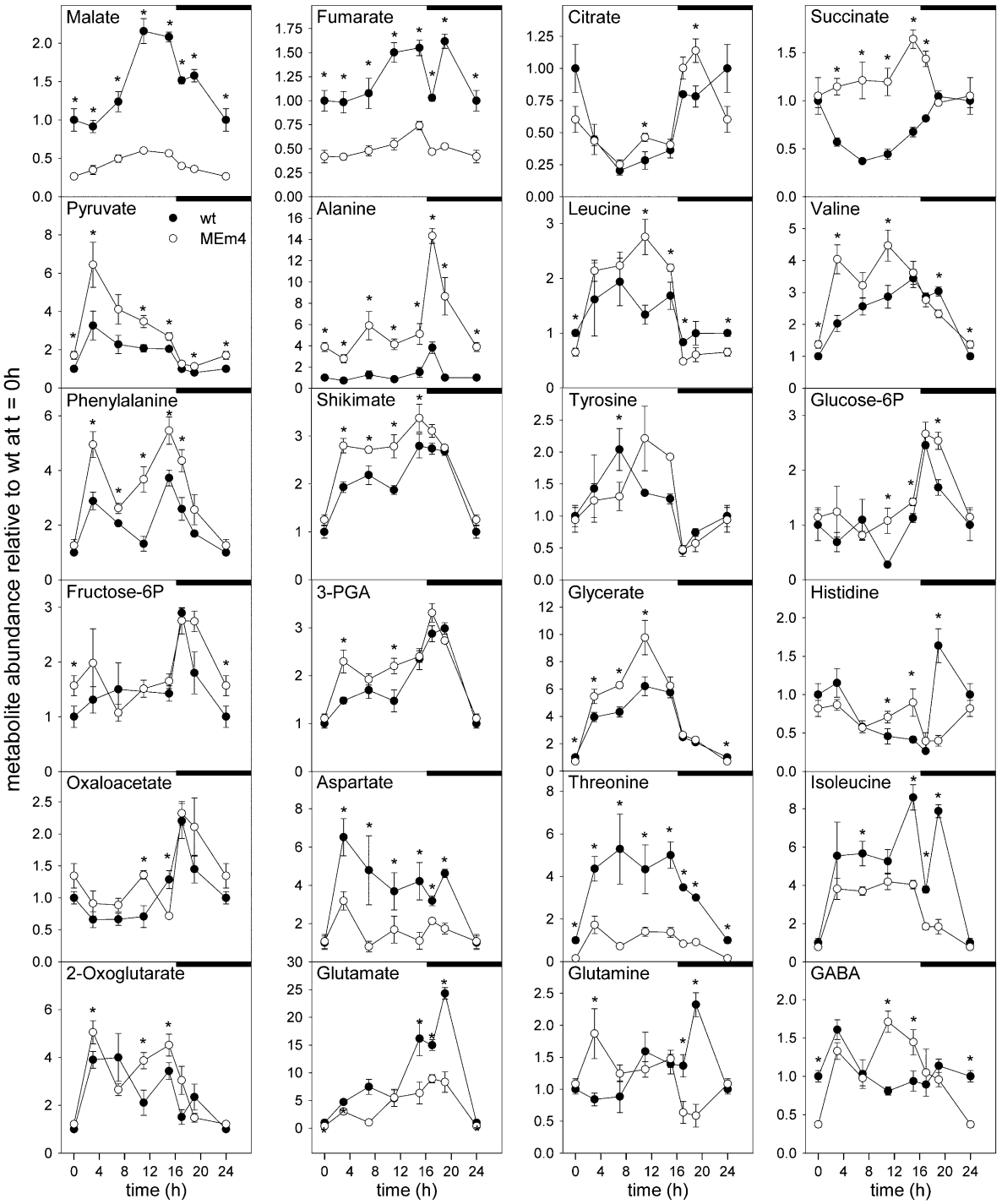

Figure 3. Diurnal metabolic changes assayed by GC-MS in MEm transformants (MEm4; open circles) and the wild type (closed circles) grown in a 16-h-light/8-h-night regime. Samples were taken at the time points indicated in the "Materials and Methods." In each graphic, the wild-type level at the end of the night period (t = 0 h) was set to 1 and the *y* axis represents metabolite levels relative to it. Values presented are mean ± SE of replicates of five plants each. The asterisk (*) indicates significant differences between the values of the wild type and MEm4 calculated by Student's *t* test ($P < 0.05$). The night period is highlighted with black bars.

type (Fig. 3). In both cases, the levels increased after the onset of the night period and decreased again to minimal levels by the end of the night. 3-Phosphoglycerate (3-PGA) and glycerate accumulated during the light phase in all lines, but the transgenics presented higher levels than the wild type (Fig. 3). While glycerate levels

constantly decreased during the night period, those of 3-PGA increased further during the first hours in dark and then decreased steeply to reach the lowest levels by the end of the night phase (Fig. 3). PEP is produced from 3-PGA and its condensation with erythrose-4-P gives rise to the shikimate pathway, in which the aromatic amino acids are synthesized. In the MEm transformants, shikimate and Phe levels were significantly higher than in the wild type throughout the day period, while Tyr levels were not significantly different (Fig. 3). Trp levels remained consistently beneath detection levels.

MEm Transgenic Lines Show Accelerated Dark-Induced Senescence

Metabolic alterations encountered in the MEm transgenic plants, such as low levels of metabolites that could be used as respiratory substrates, toward the end of the dark period led us to investigate the response of these plants to carbon starvation. One of the most efficient stimuli that accelerate sugar starvation is the inhibition of photosynthesis (Brouquisse et al., 1998). Thus, 4-week-old plants growing under long days were separated into two sets. One set was kept in long days, and the second set was kept in darkness to induce natural sugar starvation and, thus, dark-induced senescence. Dark-induced senescence occurred slowly in the wild type, where yellowing was obvious after 6 d of darkness. In contrast, in the transgenic lines, a dramatic reduction in their ability to withstand extended darkness was observed. Senescence already initiated after 3 d and showed dramatic yellowing after 4 d of dark treatment (Fig. 2A). In the wild type and the MEm transformants, the yellowing pattern progressed like in normal senescence, in which the distal part of the leaves senesce first and the tissue surrounding the veins stays longer green to maximize transport from the leaf (Buchanan-Wollaston et al., 2005).

To further investigate the progress of the dark-induced senescence in the MEm plants, some senescence markers were investigated. Two parameters related to chloroplast function, total chlorophyll (Fig. 2B) and the photochemical efficiency of PSII (F_V/F_M value; Fig. 2C), showed a more rapid decay in the transgenic lines. The total protein concentration (Fig. 2D) and the content of the Rubisco large-subunit polypeptide analyzed by SDS-PAGE (Fig. 2E) also declined earlier in the MEm plants. Evans blue staining was used as indicator of cell death. As shown in Figure 2F, higher rates of cell death were observed in all transgenic lines as compared to the wild type. All these results indicate that the onset and progress of dark-induced senescence is more rapid in the MEm transgenic plants.

Metabolite Profiling during Dark-Induced Senescence

To better characterize the influence of enhanced chloroplastic NADP-ME activity on leaf metabolism, rosettes from 4-week-old plants grown in long days were harvested at different time points during prolonged dark treatment and subjected to metabolic analysis.

At the end of the night period, the content of starch, Suc, Glc, and Fru reached a minimum in all MEm transgenic and wild-type plants (Supplemental Table S1). When the plants were maintained in constant darkness, the levels of starch and Suc decreased rapidly during the first hours of treatment, reaching minimum levels after 30 h in darkness (Supplemental Table S1; Fig. 4). MEm transformants showed no differences in the amount and degradation rate of starch and Suc as compared to the wild type during dark-induced senescence (Supplemental Table S1; Fig. 4). Similarly, Glc and Fru contents decreased during the first hours in permanent darkness and stayed at low levels afterward (Fig. 4; Supplemental Tables S1 and S3). Sugars such as Gal and gluconate were maintained at very low levels in prolonged darkness until day 6, from which point they increased sharply (Fig. 4; Supplemental Table 3).

Malate, fumarate, citrate, succinate, and 2-oxoglutarate decreased during the first hours in constant darkness to a minimum that was maintained during the next days (Fig. 4; Supplemental Table S3). By day 4 the MEm transformants showed an increase in the content of these metabolites, while in the wild type similar increases were observed by day 6. Other metabolites that showed a similar pattern were glycerate and shikimate (Fig. 4). However, in both cases, the increments were not as pronounced as those of the intermediates of the TCA cycle (Fig. 4). In contrast, pyruvate levels decreased in the first hours of darkness and were maintained at low levels throughout the period analyzed (Fig. 4). The contents of pyruvate in the MEm lines were always higher than those of the wild type.

The metabolic profiles of individual amino acids were followed during 7 d in continuous darkness. In the wild type and the MEm transformants, Ala showed an increment during the first hours in continuous darkness and decreased afterward to reach minimum values by day 2 (Fig. 4). In the wild type, this minimum level was maintained during the next 3 d and slightly increased again by day 6, while in the MEm plants a pronounced increment occurred again by day 4 (Fig. 4). In both cases, the second increment in Ala levels was temporally correlated with the appearance of the first symptoms of senescence.

Glu and Asn showed almost the same profile in the wild type and the MEm transformants during the first 4 d in continuous darkness. Glu levels increased after 24 h in darkness, dropped during the next day, and afterward increased further (Fig. 4). In the case of the MEm plants, the highest accumulation was achieved by day 5, with levels dropping afterward again. In the wild type, two maxima were recorded, one at day 4 and the second at day 7. Asn levels were at the limit of detection during the first day in darkness but increased steadily after 24 h, with maximum levels at the same time points as for Glu (Fig. 4). Gln showed the

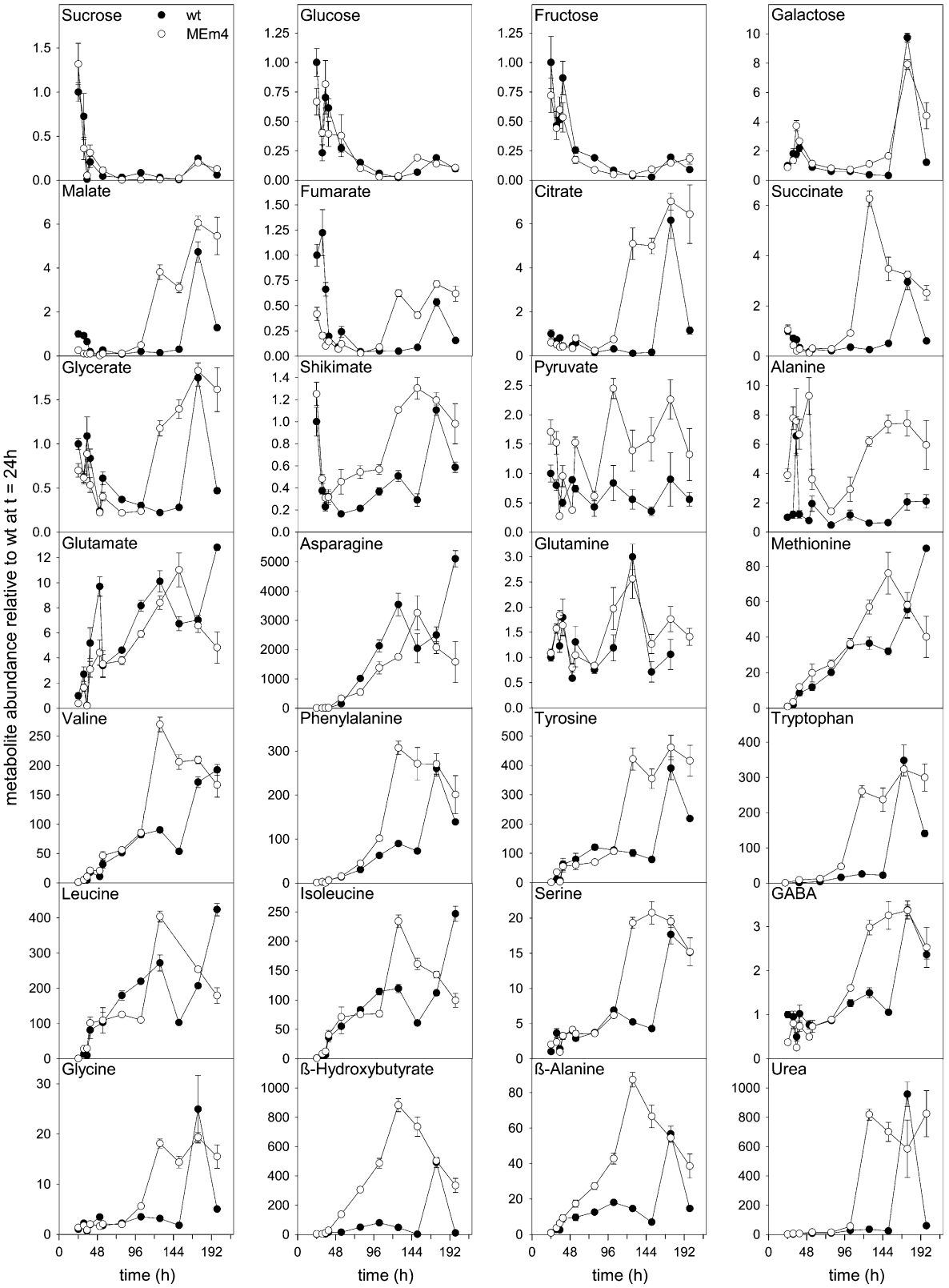

Figure 4. Metabolic changes assayed by GC-MS in MEm transformants (MEm4, open circles) and the wild type (closed circles) during extended dark conditions. Samples were taken at the time points indicated in the "Materials and Methods." The *x* axis starts at the end of a complete diurnal cycle. In each graph, the wild-type level at the end of the night period was set to 1 and the *y* axis represents metabolite levels relative to it. Values presented are means ± SE of replicates of five plants each.

same profile in the MEm plants and the wild type. Two small peaks with almost the same maxima were observed at 15 h and 4 d in darkness, respectively (Fig. 4).

A constant increase in the levels of Met, Val, Phe, Tyr, Trp, Leu, Ile, and Ser was observed directly after the onset of continuous darkness. By day 4, the levels of these amino acids increased rapidly and reached the highest values in the MEm plants, while in the wild type the maximum levels were observed by day 6 (Fig. 4). GABA and Gly maintained low levels during the first day in darkness and highly increased by day 4 in the MEm plants, while in the wild type the same increase occurred by day 6 (Fig. 4). Two metabolites that presented a similar pattern as the majority of the amino acids are β-hydroxybutyrate and β-Ala, whereas urea and Rib mirrored the pattern of Gly (Fig. 4; Supplemental Table S3).

We next measured the levels of adenylates since the energy charge has long been postulated to influence senescence and it has recently been demonstrated that a limitation of nocturnal import of ATP into the chloroplast leads to severe problems in plastidial metabolism (Reinhold et al., 2007). However, a change in the levels of ATP or ADP could not be observed in the transformants (data not shown).

Metabolic Complementation of Dark-Induced Senescence

A more rapid dark-induced senescence was obtained when 3-week-old seedlings growing in solid medium were transferred to Whatman filter paper imbibed in water and maintained in continuous darkness. In this case, wild-type plantlets and MEm transformants entered senescence 4 and 2 d after dark incubation, respectively. We investigated whether the rapid dark-induced senescence observed in the MEm plants could be compensated for by an exogenous supply of metabolites that could serve as energy source. To test this hypothesis, the plantlets, transferred to Whatman filter paper, were imbibed in solutions of different metabolites and maintained in continuous darkness. As shown in Figure 5, exogenously supplied Glc, Suc, and L-malate avoided the premature in vitro dark-induced senescence of the transgenic MEm lines, while fumarate and D-Glu compensated for at least a part of it. No complementation of the phenotype could be observed by the supply of L-Leu or L-Val (not shown).

To reveal some metabolic changes that could account for the complementation observed, a metabolic profile of plantlets maintained in water or supplemented with Glc was conducted by GC-MS after 3 d of incubation in darkness. When the seedlings were maintained in water, significantly lower levels of malate, fumarate, 2-oxoglutarate, and Asn were observed in all MEm transformants (Fig. 6). Ala, Val, Ser, Ile, Trp, and Tyr accumulated significantly in at least two MEm lines and Phe showed the same tendency, while Suc, the free sugars, and the phosphorylated forms were

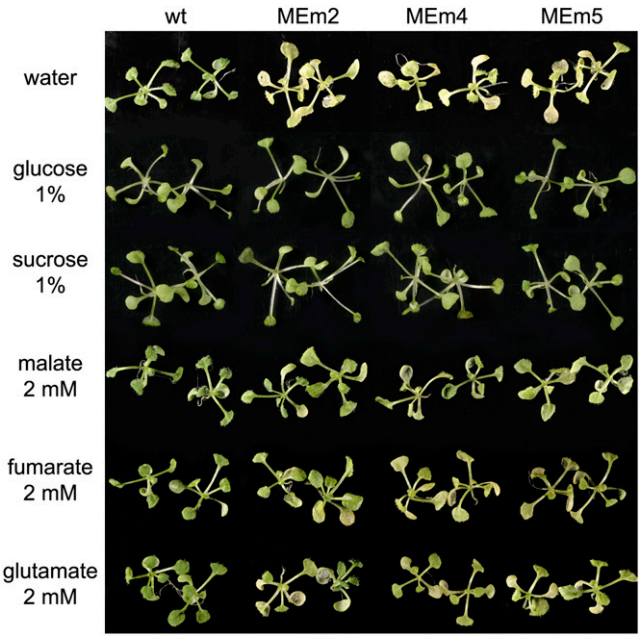

Figure 5. Complementation of the MEm phenotype in dark-induced senescence. Three-week-old seedlings grown on solid media were placed onto Whatman filter papers containing water, 1% Glc, 1% Suc, 2 mM malate, 2 mM fumarate, or 2 mM Glu and kept in darkness for 3 d.

similar in both the MEm transformants and the wild type (Fig. 6; Supplemental Table S4). Other metabolites measured showed comparable levels in the wild type and the MEm transformants, like in the case of Glu and GABA (Fig. 6; Supplemental Table S4).

When plants supplied with Glc were incubated 3 d in darkness, the contents of malate and fumarate in the wild type increased 1.2- and 2.7-fold, respectively, as compared with the levels present in the plants maintained in water (Fig. 6). In MEm transformants, the contents of malate and fumarate increased 5- to 6-fold as compared to the levels found in the MEm lines incubated in water (Fig. 6). It is interesting to note that these levels were comparable or even higher than those found in the wild type incubated in water, a condition where senescence in the wild type was not evident (Fig. 6).

In comparison with the levels found in the wild type incubated with water, the same plantlets supplemented with Glc showed a decreased level of 2-oxoglutarate but a similar content of Asn (Fig. 6). In MEm lines supplied with Glc, the contents of these two metabolites were comparable to the wild type in the same condition for 2-oxoglutarate but remained low for Asn (Fig. 6). On the other hand, after dark incubation with Glc, Val, Trp, and Phe were at similar levels in the MEm transformants and the wild type, while Ile and Tyr were even lower in the MEm lines (Fig. 6). Interestingly, Ala and Ser accumulated to high levels in at least two of the MEm transformants, probably synthesized from pyruvate, the product of the NADP-ME reaction (Fig. 6). As expected, the levels of Suc and the

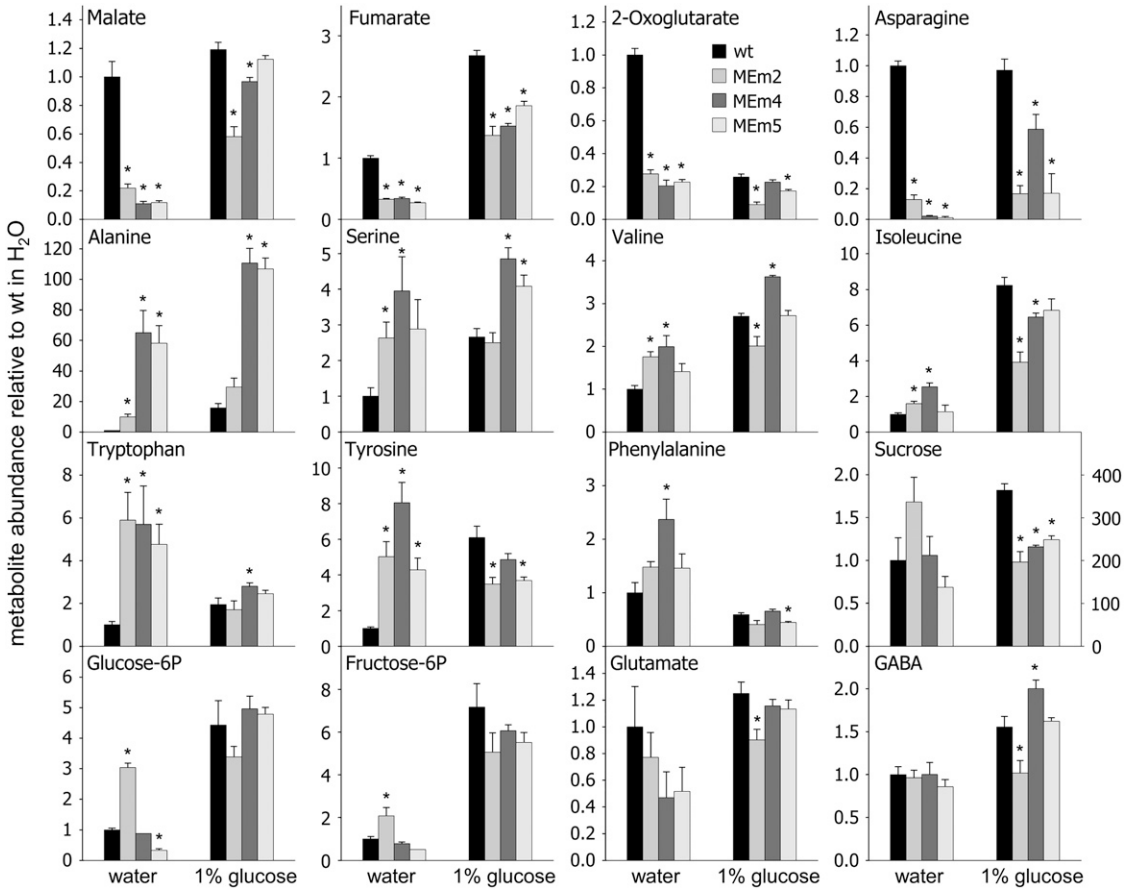

Figure 6. Metabolic changes assayed by GC-MS in MEm transformants and the wild type during the complementation assays. Values presented are means ± SE of two replicates of pools of at least 20 plantlets each. An asterisk (*) indicates significant differences to corresponding wild-type values calculated by Student's *t* test ($P < 0.05$). In the Suc panel, the scale at the right refers to data obtained after Glc feeding.

free and phosphorylated sugar forms increased considerably after Glc feeding and were similar in both the MEm transformants and the wild type after 3 d in the dark supplemented with Glc (Fig. 6).

DISCUSSION

The constitutive expression of the maize C_4 NADP-ME in Arabidopsis chloroplasts was successfully achieved. The transgenic lines showed a range of NADP-ME activities that positively correlated with the amount of an immunoreactive 62-kD protein observed in the immunoblot analysis (Fig. 1). Furthermore, the correct processing of the in vitro synthesized NADP-ME precursor protein was demonstrated by import experiments into isolated chloroplasts and by immunocytochemical studies on leaf sections of transgenic and wild-type lines (Fig. 1). Moreover, native gel electrophoresis of leaf extracts stained for NADP-ME activity indicated that the maize mature NADP-ME was correctly assembled in Arabidopsis chloroplasts. In contrast to the results obtained here, Takeuchi et al. (2000) were unable to obtain overexpression of a maize NADP-ME in rice (*Oryza sativa*) despite using the same promoter (cauliflower mosaic virus [CaMV] 35S) that was used in this study. However, rice plants expressing maize C_4 NADP-ME under the rice cab promoter showed serious deteriorative effects on growth, such as bleaching of leaves and growth hindrance under autotrophic conditions (Takeuchi et al., 2000; Tsuchida et al., 2001). These findings contrast with the results presented here where the overexpression of the maize C_4 NADP-ME in Arabidopsis led to no visible phenotypic changes in plants grown in long days and under normal light conditions (Fig. 2). Laporte et al. (2002) have also shown that the expression of NADP-ME in tobacco (*Nicotiana tabacum*) under the control of the strong constitutive mas (mannopine synthase) promoter did not result in phenotypic changes, but the transgenic plants showed a decreased stomatal conductance. As Arabidopsis is a dicotyledonous species and rice is a monocotyledonous one, the introduction of the highly active C_4 NADP-ME might have induced different physiological disturbances in each species, most probably due to the metabolic differences encountered

among these plants. In this regard our results indicated that fumarate accumulates to high levels during the light period in Arabidopsis wild-type plants. Moreover, Chia et al. (2000) previously described a high fumarate accumulation and measured concentrations up to several milligrams per gram fresh weight in Arabidopsis leaves, which were in the same range as those of sugars. These authors also found that, besides Arabidopsis, a number of other C_3 species accumulate high levels of fumaric acid in photosynthetically active tissues, predominantly at the end of the light period. In rice, only very low levels of fumaric acid were detected. Furthermore, in long-day conditions we have not observed differences between the MEm plants and the wild type in the F_V/F_M ratio (an indicator of photoinhibition), the activation state of NADP-MDH (an indicator of the NADP/NADPH ratio; not shown), and the total glutathione and ascorbate levels (not shown) during the day period. In contrast, the overexpression of NADP-ME in rice resulted in severe bleaching, decreased F_V/F_M ratio, and an increased NADP-MDH activation state. This increased photoinhibition was suggested to be a consequence of increased NADPH levels (Tsuchida et al., 2001). All the above-cited results suggest that, at least in Arabidopsis, metabolic flexibility ensures the capacity to remove possible deleterious alterations in the redox status caused by the overexpression of NADP-ME in plastids.

The MEm plants analyzed in this study showed an informative metabolic phenotype, i.e. severe metabolic alterations with respect to the wild-type plants that could be attributed to the enhanced activity of NADP-ME. Malate levels were dramatically decreased during the entire diurnal period and almost stayed constant at a low level during the day (Fig. 3). Thus, the typical malate accumulation at the end of the day period was not observed in the MEm transformants. Exactly the same pattern was observed for fumarate, indicating a tight relationship between both organic acids. The parallel decrease of malate and fumarate observed in the MEm plants is most probably due to the action of fumarase catalyzing a reaction that is presumed to operate close to the thermodynamic equilibrium in vivo.

It is interesting to note that the maximum levels of both malate and fumarate in the MEm plants at the end of the light period were approximately the same as the minimum levels found in the wild type at the end of the night period. This indicates that in MEm transformants both metabolites were permanently below the normal concentrations found in illuminated leaves of the wild type. Pyruvate, the product of the NADP-ME reaction, was slightly increased at the end of the night period and accumulated in the light phase in the MEm transformants, very likely as a consequence of the high NADP-ME activity (Fig. 3). Metabolites that are derived from pyruvate, such as Ala, Leu, and Val, were also substantially increased in the overexpressors, while diurnal changes in sugar and starch levels are in agreement with those described previously (Gibon et al., 2004; Bläsing et al., 2005).

The main purpose of senescence in green plants is the mobilization and recycling of nutrients that had been produced in the leaves and that are being transferred to other parts of the plant. Developmental signals, aging, stress, and darkness all can induce senescence. When plants are placed in the dark, the loss of photosynthetically fixed carbon results in a rapid depletion of the sugar levels in the leaves (Brouquisse et al., 1998; Tcherkez et al., 2003). The ensuing low carbohydrate levels induce expression of senescence-associated genes in Arabidopsis and initiate substantial changes in physiological and biochemical processes with the aim to sustain respiration and other metabolic processes (van Doorn, 2004). Dark-induced senescence, due to this carbon starvation, occurs slowly in intact plants (Lin and Wu, 2004). Chlorophyll degradation is the first visible symptom of senescence, and proteolysis of chloroplast proteins (principally Rubisco) begins at early phases of senescence, leading to a decline of photosynthetic capacity. All these events obviously occurred earlier in the MEm transformants relative to the wild type and correlated with the accelerated appearance of visible yellowing and premature death observed in these plants (Fig. 2). Many metabolites typically increase in senescing leaves. It was reported that PPDK expression is significantly up-regulated after the onset of dark-induced senescence (Graham et al., 1992; MacLaughlin and Smith, 1994; Lin and Wu, 2004), being involved in the production of metabolic precursors for the synthesis of Asn, which is primarily mobilized in dark-induced senescence, while Gln is the metabolite used in nitrogen remobilization during developmental senescence (Lin and Wu, 2004; Buchanan-Wollaston et al., 2005). The increase in Asn has been related to the storage of nitrogen released by the degradation of proteinogenic amino acids under carbohydrate starvation since accumulation of NH_4^+ is toxic for the cell (Givan, 1979). Brouquisse et al. (1998) described that, after 48 h of darkness, Asn increased by a factor of 18 and Gln dropped in young leaves of Arabidopsis. Our results showed that both the wild type and the MEm lines contained significantly increased contents of Asn, while Gln levels were only slightly enhanced after the onset of prolonged darkness (Fig. 4). We also observed that the levels of branched-chain amino acids, i.e. Leu, Ile, and Val, increased during the dark treatment. Genes involved in branched-chain amino acid catabolism were found to be up-regulated in dark-induced senescence but not during developmental senescence (Fujiki et al., 2001). Interestingly, knockout mutants of the electron transfer flavoprotein/electron transfer flavoprotein ubiquinone oxide reductase electron transport complex, which is involved in the degradation of branched-chain amino acids, also display an accelerated dark-induced senescence (Ishizaki et al., 2005, 2006). Catabolism of branched-chain amino acids via β-oxidation provides alternative respiratory substrates under carbohydrate deprivation. During the progress of senescence and as a result

of protein breakdown, the levels of Phe, Tyr, and Trp also increased markedly. Our results showed dramatic increases of these metabolites at the same times that yellowing was evident in the transformants and the wild type, suggesting that such changes are indicative for extreme senescence (Figs. 2 and 4).

Intriguingly, while the MEm transformants showed similar general patterns of metabolic changes as the wild type in response to extended darkness, all the above-mentioned metabolites rose 2 to 3 d earlier in the MEm transformants than in the wild type (Fig. 4). Thus, the metabolic consequences originating from prolonged darkness are induced earlier in the MEm transformants. The comparative analysis of the metabolic profiles in correlation with the severity of senescence symptoms in the MEm lines and the wild type allowed us to identify putative markers of metabolic senescence. With the onset of senescence, drastic changes in leaf metabolism occurred, and Leu, Ile, Val, Phe, Tyr, Trp, and urea all increased to much higher levels than those observed during a normal diurnal period. The increments determined were similar for MEm lines and the wild type, indicating that they are exclusively related to protein breakdown and organic nitrogen recycling activated during the senescence process. Moreover, MEm lines kept in the dark on Whatman filter paper soaked with water entered senescence already after 2 d and showed enhanced accumulation of the senescence marker metabolites Ile, Val, Phe, Tyr, and Trp. However, prematurely induced senescence could be prevented and wild-type metabolite levels could be maintained by supplying MEm transformants with Glc, Suc, or malate, i.e. with a metabolite that can be used as a readily mobilized energy source (Figs. 5 and 6).

In line with these results, malate and fumarate were the only two metabolites whose levels were significantly decreased in the MEm lines after dark incubation and whose levels recovered to values similar to the wild-type ones after incubation with Glc. Such changes were not observed for other metabolites, e.g. Ala, Asn, or 2-oxoglutarate. Taken together, these results provide strong evidence that the low levels of malate and fumarate are involved in and causally related to the accelerated dark-induced senescence phenotype observed in the MEm transformants. Further studies on the regulation of sugar and carbon fluxes in Arabidopsis will reveal the function of these metabolites as transient storage forms of fixed carbon and energy.

MATERIALS AND METHODS

Plant Material, Growth Conditions, and Sampling

After a cold treatment of 48 h at 4°C in the dark, Arabidopsis (*Arabidopsis thaliana*) 'Columbia-0' (wild type) and the transgenic lines were grown under long-day conditions (16 h light/8 h night) at a photosynthetically active photon flux density of 70 to 100 μmol quanta m^{-2} s^{-1}. During the day, the temperature was 22°C and during the night 18°C. For dark treatments, 4-week-old plants were kept in the same growth chamber in complete darkness. Complete rosettes were harvested, transferred immediately into liquid nitrogen, and stored at −80°C until further analysis. Samples for metabolite measurements during a diurnal cycle were taken beginning at the end of the night period (t = 0 h), and 3, 7, 11, 15, 17, 19, 21, and 24 h later. For the prolonged dark treatment, samples were collected beginning at the end of the first night period (t = 24 h), and 31, 35, 39, 51, 55, 79, 103, 127, 151, 175, and 199 h later. Material from four to six different plants were combined per sample. All measurements were repeated with at least four different samples and two independent biological replicates.

For the complementation assays, plantlets were grown on Murashige and Skoog media containing 1% Suc under long-day conditions (16 h light/8 h night) at a photosynthetically active photon flux density of 75 μmol quanta m^{-2} s^{-1}. After 3 weeks, plantlets were transferred to Whatman filters soaked alternatively with water, 1% Suc, 1% Glc, 2 mM L-malate, 2 mM L-fumarate, 2 mM D-Glu, 2 mM L-Leu, or 2 mM D-Val, and were kept in darkness. After 3 d, the rosettes were harvested and immediately frozen in liquid nitrogen and stored at −80°C until further analysis.

Plasmid Construction and Plant Transformation

Full-length cDNA encoding the maize (*Zea mays*) C_4 NADP-ME precursor protein (Detarsio et al., 2003) was cut out from pBluescript using the *Sac*II and *Kpn*I sites and blunt-ended using the Klenow fragment of DNA polymerase. The 2.2-kb fragment was cloned into a modified version of the binary vector pGreenII bearing the BASTA resistance gene (Hellens et al., 2000), using the *Sma*I site between the CaMV 35S promoter and the octopin synthetase terminator from the pBinAR vector (Bevan, 1984). Unique cloning sites of the basic pGreenII vector, which interfered with the next cloning steps (*Kpn*I, *Sal*I, *Eco*RV, *Pst*I, *Sma*I, *Bam*HI, *Spe*I, and *Xba*I), were eliminated by cutting with the corresponding restriction enzymes, blunting, and religating. The multiple cloning site, the CaMV 35S promoter, and the octopin synthetase terminator from the pBinAR vector (529 bp) were cloned into the pGreenII-nosBAR *Eco*RI and *Hin*dIII sites. The resulting modified version of the pGreenII vector was called pGreenII-35S-nosBAR, and the plasmid containing the maize C_4 NADP-ME was called *35S:MEm*C_4.

The plasmid *35S:MEm*C_4 was introduced into Arabidopsis by *Agrobacterium tumefaciens* (GV3101)-mediated transformation using the vacuum-infiltration method (Bechtold et al., 1993). Transformants were selected for resistance to BASTA. DNA was extracted from leaf material collected from selected plants and used for PCR analyses. Plants containing the transgene were transplanted and allowed to self-pollinate. Seeds from the primary (T1) generation were sown, and resultant T2 plants were subjected to another round of BASTA selection and characterization by means of PCR and NADP-ME activity assay. The process was repeated to obtain nonsegregating T3 transgenic lines. All further analyses were performed with homozygous T3 transgenic plants.

Southern Blot

Genomic DNA was isolated from leaves and digested with *Eco*RI. The blot was hybridized with a 1.1-kb fragment corresponding to the BASTA resistance gene, using standard conditions (Sambrook et al., 1989). Washes were carried out at low stringency (2× SSC and 1× SSC, 0.1% SDS at 65°C).

Chloroplast Import

The full-length maize C_4 NADP-ME clone (Detarsio et al., 2003) was transcribed and translated in vitro using the TNT-coupled reticulocyte lysate system and ^{35}S-Met as labeled amino acid according to the manufacturer's instructions (Promega). The resulting radiolabeled precursor protein was used in a plastid import assay using isolated spinach (*Spinacia oleracea*) chloroplasts. After import, the washed chloroplasts were split into two aliquots and one of them was treated with thermolysin (0.1 mg/mL). All samples were run on a 10% SDS-PAGE (Laemmli, 1970) and analyzed by fluorography.

In Situ Immunolocalization Assay

For in situ immunolocalization studies, the samples were embedded in LR gold acrylic resin. Sections (0.8 μm thick) were dried onto silane-coated slides

and incubated for 1 h with TBST/BSA (10 mM Tris-HCl, pH 7.2; 150 mM NaCl; 0.1% [v/v] Tween 20 plus 1% [w/v] BSA) to block nonspecific protein binding on the sections. The slides were then incubated for 2 h with serum against the spinach Rubisco large subunit diluted 1:1,000 or for 4 h with affinity-purified antibodies against recombinant maize NADP-ME (Saigo et al., 2004). As control, the slides were incubated for 4 h with the corresponding preimmune serum with TBST/BSA. After extensive washing with TBST/BSA, the sections were treated for 1 h with protein A-gold (15 nm; Amersham) diluted 1:100 with TBST/BSA. The slides were washed with TBST/BSA, TBST, and distilled water prior to exposition to a silver enhancement reagent according to the manufacturer's instructions (Amersham) and stained with 0.25% (w/v) Safranin O. Results were documented using a microscope (Nikon Eclipse E800) equipped with a digital camera (KY-F1030; JVC).

Extraction of Leaf Soluble Protein

Leaf material of 6-week-old Arabidopsis plants were ground in liquid nitrogen and the resulting powder was suspended in 100 mM Tris-HCl, pH 7.5, 5 mM $MgCl_2$, 2 mM EDTA, 10% (v/v) glycerol, and 10 mM 2-mercaptoethanol, in the presence of a protease inhibitor cocktail (Sigma). The homogenates were clarified by centrifugation and the supernatants were separated for activity measurements or prepared for electrophoresis.

Enzymatic Assays

NADP-ME activity was determined spectrophotometrically using a standard reaction mixture containing 50 mM Tris-HCl, pH 8.0, 10 mM $MgCl_2$, 0.5 mM NADP, and 10 mM L-malate in a final volume of 0.5 mL. The reaction was started by the addition of L-malate. One unit (U) is defined as the amount of enzyme that catalyzes the formation of 1 μmol NADPH min^{-1} under the specified conditions.

Protein Detection and Identification

Protein samples were analyzed by SDS-PAGE (10% [w/v] according to Laemmli [1970]). Proteins were visualized with Coomassie Blue or electroblotted onto a nitrocellulose membrane for immunoblotting. Antibodies against the recombinant maize photosynthetic NADP-ME (Detarsio et al., 2003) were used for detection (1:100). Bound antibodies were visualized by linking to alkaline phosphatase-conjugated goat anti-rabbit IgG according to the manufacturer's instructions (Sigma). Alkaline phosphatase activity was detected colorimetrically. Native PAGE was performed using a 6% (w/v) acrylamide separating gel. Electrophoresis was run at 150 V at 10°C. Gels were assayed for NADP-ME activities by incubating the gel in a solution containing 50 mM Tris-HCl, pH 7.5, 10 mM L-malate, 10 mM $MgCl_2$, 0.5 mM NADP, 35 mg/mL nitroblue tetrazolium, and 0.85 μg/mL phenazine methosulfate at 30°C.

Measurement of Senescence Parameters

Chlorophyll was extracted from leaf samples by grinding in 96% ethanol. Following pelleting debris by centrifugation, chlorophyll *a* and chlorophyll *b* contents were determined essentially as described by Wintermans and De Mots (1965). Protein was quantified by the Bradford assay (Bradford, 1976).

Chlorophyll fluorescence measurements were performed with a PAM-2000 pulse amplitude-modulated chlorophyll fluorometer (Walz GmbH). At the start of each measurement, a plant was dark adapted for 10 min. Basal fluorescence (F_0) was measured with modulated weak red light and maximum fluorescence (F_m) was induced with a saturating white light pulse (5,000 mmol m^{-2} s^{-1}; duration 0.8 s).

Estimation of Cell Death

Detached leaves were incubated in a 0.1% (w/v) Evans blue aqueous solution, vacuum infiltrated during 5 min and washed three times with distilled water. The dye bound to the dead cells was removed by incubation in 50% (v/v) methanol and 1% SDS at 60°C and quantified spectrophotometrically at 600 nm. For each sample leaves of six independent plants were pooled. Cell death in detached leaves, was visualized by Evans blue staining followed by removal of chlorophylls. The leaves were fixed with 50% (v/v) ethanol, 5% (v/v) acetic acid and 3.7% (v/v) formaldehyde and photographed.

Determination of Metabolite Levels by GC-MS

For GC-MS analysis, polar metabolites were extracted with MeOH/$CHCl_3$ from 100 mg of complete rosettes ground previously to a fine powder. Metabolite samples were derivatized by methoxyamination, using a 20 mg/mL solution of methoxyamine hydrochloride in pyridine, and subsequent trimethylsilylation with MSTFA. An aliquot of the derivate was injected into a GC-MS system (AS 7683 autosampler, GC 6890N gas chromatograph, and MS 5973N mass spectrophotometer; Agilent). Signals were normalized to an internal standard molecule introduced to the samples (ribitol), allowing a relative quantification of metabolites. The chromatograms and mass spectra were evaluated using the G1701DA MSD Productivity ChemStation software (Agilent).

Quantification of Carbohydrates and Fumarate

The frozen samples were extracted two times for 15 min in 0.75 mL of 80% (v/v) ethanol at 70°C. The extracts were combined, dried down under vacuum, and dissolved in 0.5 mL of water. The contents of Glc, Fru, and Suc were determined enzymatically according to Stitt et al. (1989). For the determination of starch, the ethanol-insoluble material was homogenized in 0.2 mL KOH (0.2 N). The suspension was adjusted to pH 5.5 with 1 N HAc and incubated overnight with 3.5 U α-amylase and 2.5 U amyloglucosidase at room temperature. The digested material was incubated 5 min at 95°C, centrifuged, and the Glc content of the resulting supernatant determined as described above. Fumarate content of 4-week-old wild-type rosette leaves at the end of the light period was measured spectrophotometrically using the combined assay as in Hurth et al. (2005).

Nucleotide Measurements

Nucleotides were extracted by grinding frozen leaf material (approximately 100 mg) with liquid nitrogen followed by extraction in trichloroacetic acid. Adenylates were separated and measured by HPLC as described by Fernie et al. (2001).

Sequence data from this article can be found in the GenBank/EMBL data libraries under accession number J05130.

Supplemental Data

The following materials are available in the online version of this article.

Supplemental Table S1. Complete data set of starch and soluble sugars measured by end-point enzymatic assays over a long-day diurnal cycle and dark-induced senescence.

Supplemental Table S2. Complete data set of metabolites of rosettes over a long-day diurnal cycle.

Supplemental Table S3. Complete data set of metabolite of rosettes during dark-induced senescence.

Supplemental Table S4. In vitro metabolic complementation assays.

ACKNOWLEDGMENTS

We thank Dr. Nele Horemans for performing the HPLC measurements of ascorbate and glutathione, and Claudia Nothelle and Ulrike Hebbeker for technical assistance.

Received June 22, 2007; accepted September 14, 2007; published September 20, 2007.

LITERATURE CITED

Bechtold N, Ellis J, Pelletier G (1993) *In planta* Agrobacterium mediated gene transfer by infiltration of adult *Arabidopsis thaliana* plants. C R Acad Sci III Sci Vie **316:** 1194–119

Bevan M (1984) Binary Agrobacterium vectors for plant transformation. Nucleic Acids Res **12:** 8711–8721

Bläsing OE, Gibon Y, Günther M, Höhne M, Morcuende R, Osuna D, Thimm O, Usadel B, Scheible WR, Stitt M (2005) Sugars and circadian regulation make major contributions to the global regulation of diurnal gene expression in *Arabidopsis.* Plant Cell **17:** 3257–3281

Bradford MM (1976) A rapid and sensitive for the quantitation of microgram quantities of protein utilizing the principle of protein-dye binding. Anal Biochem **72:** 248–254

Brouquisse R, Gaudillère JP, Raymond P (1998) Induction of a carbon-starvation-related proteolysis in whole maize plants submitted to light/dark cycles and to extended darkness. Plant Physiol **117:** 1281–1291

Buchanan-Wollaston V, Page T, Harrison E, Breeze E, Lim PO, Nam HG, Lin JF, Wu SH, Swidzinski J, Ishizaki K, et al (2005) Comparative transcriptome analysis reveals significant differences in gene expression and signalling pathways between developmental and dark/starvation-induced senescence in Arabidopsis. Plant J **42:** 567–585

Chia DW, Tenessee JY, Retier WD, Gibson S (2000) Fumaric acid: an overlooked form of fixed carbon in Arabidopsis and other plant species. Planta **211:** 743–751

Detarsio E, Gerrard Wheeler MC, Campos Bermúdez VA, Andreo CS, Drincovich MF (2003) Maize C_4 NADP-malic enzyme. Expression in *Escherichia coli* and characterization of site-directed mutants at the putative nucleotide-binding sites. J Biol Chem **278:** 13757–13764

Drincovich M, Casati P, Andreo CS (2001) NADP-malic enzyme from plants: a ubiquitous enzyme involved in different metabolic pathways. FEBS Lett **490:** 1–6

Emmerlich V, Linka N, Reinhold T, Hurth MA, Traub M, Martinoia E, Neuhaus HE (2003) The plant homolog to the human sodium/dicarboxylic cotransporter is the vacuolar malate carrier. Proc Natl Acad Sci USA **100:** 11122–11126

Fernie AR, Roscher A, Ratcliffe RG, Kruger N (2001) Fructose 2,6-bisphosphate activates pyrophosphate: fructose-6-phosphate 1-phosphotransferase and increases triose phosphate to hexose phosphate cycling in heterotrophic cells. Planta **212:** 250–263

Fontaine V, Hartwell J, Jenkins GI, Nimmo HG (2002) *Arabidopsis thaliana* contains two phosphoenolpyruvate carboxylase kinase genes with different expression patterns. Plant Cell Environ **25:** 115–122

Fujiki Y, Ito M, Nishida I, Watanabe A (2001) Leucine and its keto acid enhance the coordinated expression of genes for branched-chain amino acid catabolism in Arabidopsis under sugar starvation. FEBS Lett **499:** 161–165

Gerrard Wheeler MC, Tronconi MA, Drincovich MF, Andreo CS, Flügge UI, Maurino VG (2005) A comprehensive analysis of the NADP-malic enzyme gene family of Arabidopsis. Plant Physiol **139:** 39–51

Gibon Y, Bläsing O, Palacios N, Pankovic D, Hendriks JHM, Fisahn J, Höhne M, Günter M, Stitt M (2004) Adjustment of diurnal starch turnover to short days: A transient depletion of sugar towards the end of the night triggers a temporary inhibition of carbohydrate utilisation, leading to accumulation of sugars and post-translational activation of ADP glucose pyrophosphorylase in the following light period. Plant J **39:** 847–862

Givan CV (1979) Metabolic detoxification of ammonia in tissues of higher plants. Phytochemistry **18:** 375–382

Gout E, Bligny R, Pascal N, Douce R (1993) ^{13}C nuclear magnetic resonance studies of malate and citrate synthesis and compartmentation in higher plant cells. J Biol Chem **268:** 3986–3992

Graham I, Leaver CJ, Smith SM (1992) Induction of malate synthase gene expression in senescent and detached organs of cucumber. Plant Cell **4:** 349–357

Hellens RP, Edwards EA, Leyland NR, Bean S, Mullineaux PM (2000) pGreen: a versatile and flexible binary Ti vector for Agrobacterium-mediated plant transformation. Plant Mol Biol **42:** 819–832

Hurth MA, Suh SJ, Kretzschmar T, Geis T, Bregante M, Gambale F, Martinoia E, Neuhaus E (2005) Impaired pH homeostasis in Arabidopsis lacking the vacuolar dicarboxylate transporter and analysis of carboxylic acid transport across the tonoplast. Plant Physiol **137:** 901–910

Ishizaki K, Larson TR, Schauer N, Fernie AR, Graham IA, Leaver CJ (2005) The critical role of *Arabidopsis* electron transfer flavoprotein ubiquinone oxidoreductase during dark induced starvation. Plant Cell **17:** 2587–2600

Ishizaki K, Schauer N, Larson TR, Graham IA, Fernie AR, Leaver CJ (2006) The mitochondrial electron transfer flavoprotein complex is essential for survival of Arabidopsis in extended darkness. Plant J **47:** 751–760

Kalt W, Osmond CB, Siedow JN (1990) Malate metabolism in the dark after $^{13}CO_2$ fixation in the crassulacean plant *Kalanchoe tubiflora.* Plant Physiol **94:** 826–832

Laemmli UK (1970) Cleavage of structural proteins during the assembly of the head of bacteriophage T_4. Nature **227:** 680–685

Lance C, Rustin P (1984) The central role of malate in plant metabolism. Physiol Veg **22:** 625–641

Laporte MM, Shen B, Tarczynski MC (2002) Engineering for drought avoidance: expression of maize NADP-malic enzyme in tobacco results in altered stomatal function. J Exp Bot **53:** 699–705

Lin JF, Wu SH (2004) Molecular events in senescing Arabidopsis leaves. Plant J **39:** 612–628

MacLaughlin JC, Smith SM (1994) Metabolic regulation of glyoxylate-cycle enzyme synthesis in detached cucumber cotyledons and protoplasts. Planta **195:** 22–28

Martinoia E, Rentsch D (1994) Malate compartmentation: responses to a complex metabolism. Annu Rev Plant Physiol Plant Mol Biol **45:** 447–467

Maurino VG, Drincovich MF, Andreo CS (1996) NADP-malic enzyme isoforms in maize leaves. Biochem Mol Biol Int **38:** 239–250

Maurino VG, Saigo M, Andreo CS, Drincovich MF (2001) Non-photosynthetic malic enzyme from maize: a constitutively expressed enzyme that responds to plant defence inducers. Plant Mol Biol **45:** 409–420

Nimmo HG (2003) Control of the phosphorylation of phosphoenolpyruvate carboxylase in higher plants. Arch Biochem Biophys **414:** 189–196

Nunes-Nesi A, Carrari F, Gibon Y, Sulpice R, Lytovchenko A, Fisahn J, Graham J, Ratcliffe G, Sweetlove LJ, Fernie AR (2007) Deficiency of mitochondrial fumarase activity in tomato plants impairs photosynthesis via an effect on stomatal function. Plant J **50:** 1093–1106

Reinhold T, Aladwady A, Grimm B, Beran KC, Jahns P, Conrath U, Bauer S, Reiser J, Melzer M, Jeblink W, et al (2007) Limitation of nocturnal import of ATP into Arabidopsis chloroplasts leads to photooxidative damage. Plant J **43:** 293–304

Renné P, Dressen U, Hebbeker U, Hille D, Flügge UI, Westhoff P, Weber AP (2003) The Arabidopsis mutant *dct* is deficient in the plastidic glutamate/malate translocator DiT2. Plant J **35:** 316–321

Rothermel BA, Nelson T (1989) Primary structure of the maize NADP-dependent malic enzyme. J Biol Chem **264:** 19587–19592

Saigo M, Bologna FP, Maurino VG, Detarsio E, Andreo CS, Drincovich MF (2004) Maize recombinant non-C_4 NADP-malic enzyme: a novel dimeric malic enzyme with high specific activity. Plant Mol Biol **55:** 97–107

Sambrook J, Fritsch EF, Maniatis T (1989) Molecular Cloning: A Laboratory Manual. Cold Spring Harbor Laboratory Press, Cold Spring Harbor, NY

Scheibe R (2004) Malate valves to balance cellular energy supply. Physiol Plant **120:** 21–26

Stitt M, Lilley RMC, Gerhardt R, Heldt HW (1989) Determination of metabolite levels in specific cells and subcellular compartments of plant leaves. Methods Enzymol **174:** 518–522

Sullivan S, Shenton M, Nimmo HG (2005) Organ specificity in the circadian control of plant gene expression. Biochem Soc Trans **33:** 943–944

Takeuchi Y, Akagi H, Kamasawa N, Osumi M, Honda H (2000) Aberrant chloroplasts in transgenic rice plants expressing a high level of maize NADP-dependent malic enzyme. Planta **211:** 265–274

Taniguchi M, Taniguchi Y, Kawasaki M, Takeda S, Kato T, Sato S, Tabata S, Miyake H, Sugiyama T (2002) Identifying and characterizing plastidic 2-oxoglutarate/malate and dicarboxylate transporters in *Arabidopsis thaliana.* Plant Cell Physiol **43:** 706–717

Tcherkez G, Nogués S, Bleton J, Cornic G, Badeck F, Ghashghaie J (2003) Metabolic origin of carbon isotope composition of leaf dark-respired CO_2 in french bean. Plant Physiol **131:** 237–244

Tsuchida H, Tamai T, Fukayama H, Agarie S, Nomura M, Onodera H, Ono K, Nishizawa Y, Lee BH, Hirose S, et al (2001) High level expression of C_4-specific NADP-malic enzyme in leaves and impairment of photoautotrophic growth in a C_3 plant, rice. Plant Cell Physiol **452:** 138–145

van Doorn WG (2004) Is petal senescence due to sugar starvation? Plant Physiol **134:** 35–42

Wintermans JF, De Mots A (1965) Spectrophotometric characteristics of chlorophyll and their pheophytines in ethanol. Biochim Biophys Acta **109:** 448–453